Three-phase Magnitude-phase Detection Based on T/4 Time-lapse Elimination Method

Xiaoying Zhang
School of Electrical and Information Engineering, Lanzhou University of Technology, Lanzhou, China
Email: zhxy525@gmail.com

Zheng Jiang
School of Electrical and Information Engineering, Lanzhou University of Technology, Lanzhou, China
Email: owenronger@163.com

Ning Ding
School of Electrical and Information Engineering, Lanzhou University of Technology, Lanzhou, China
Email: dn1988518@163.com

***Abstract*—Affected by the negative sequence component and harmonic component of three-phase grid, the conventional three-phase software phase-locked loop (SPLL) circuits were unable to extract the magnitude-phase information of three-phase fundamental positive sequence component accurately, and the dynamic response speed was slow. In order to solve this problem, this paper introduces T/4 time-lapse elimination detection, a novel method of detecting three-phase magnitude-phase based on double d-q synchronous reference frame, functioning in decoupling positive and negative sequences of fundamental wave. When the voltage (or current) fundamental positive and negative sequence components are separated, the positive sequence component as well as the magnitude and phase position of negative sequence component from three-phase fundamental can be detected, so it is effective to restrain the impact on detection precision from negative sequence component. To verify the performance of this novel method, simulation experiments like transient response under normal grid condition, dynamic response under three-phase unbalance with harmonic pollution condition and dynamic response under phase jump condition are carried out. The simulation results verify that the proposed method overcomes the shortcoming of conventional three-phase phase-locked loop and tracks accurately the magnitudes and phases of the foundational positive-sequence voltage under harmonic pollution condition. And the results also verify that the proposed method can suppress odd harmonic propagation and has a higher detecting precision comparing with T/16 time-lapse elimination method. The improved T/4 time-lapse elimination detection can be wildly applied in three-phase power electronic devices.**

***Index Terms*—magnitude-phase detection; T/4 time-lapse elimination; three-phase unbalance; d-q transformation; software phase-locked loop.**

I. INTRODUCTION

Voltage converter based FACTS (Flexible Alternative Current Transmission System) devices need synchronization with power grid, and they detect the positive sequence component and negative sequence component at all times. The negative sequence component in real time is required in transformer protection and motor protection. To improve the running capacity of large grid-connected wind generation system, the frequency, phase position and magnitude of the power grid must be detected accurately and quickly [1, 2]. Due to most devices connect to the three-phase grid, three-phase phase locking and magnitude detection are especially significant. In anterior references, single phase phase-locked loop adopts hardware phase-locked method [3], tracking the phase position of power grid through zero-cross detection, but it is hard to use where harmonic pollution is heavy. At the moment, three-phase software phase-locked loop (SPLL) is widely spread and applied, and SPLL improves the importance of detecting magnitude to the same position as tracking phase position [4-10]. But affected by negative sequence and harmonic components, the phase-locked system needs select steady-state accuracy. So reducing the cut-off frequency of the loop filter is the main process, but it badly impacts the system dynamic response [7, 11]. To solve this problem, references [10, 12-14] offer modified three-phase SPLL system structures; also, references [15-19] improve the PI controller of ordinary three-phase SPLL structure, presenting various plans of controller design and parameter tuning. Besides, reference [20] introduces least squares to detect the three-phase voltages positive sequence phase position; reference [21] adopts chirp-Z transform method and reference [22] gives out a three-phase magnitude-phase-lock loop system based on extended variable step size least mean square algorithm.

Some references indicate that the previous three-phase phase-locked loop has been improved, but the dynamic response speed of grid unbalance disturbance is still greater than 1.5 frequency period [12-18]; although the dynamic response of least squares is fast, harmonic has a big impact on the steady accuracy; although Chirp-Z transform method is better than the frequency-domain analysis result of DFT(Discrete Fourier Transform), the steady-state performance of tracking line frequency is

doi:10.4304/jsw.9.2.523-529

worse than modified SPLL [11], and the extended variable step size least mean square algorithm method requires much iterative process, so the calculation amount is large.

This paper, based on dual d-q transformation, introduces a novel process to detect the three-phase magnitude and phase of the voltage. Detecting system based on this process can decouple positive and negative sequence components of fundamental wave. Also, the system can detect the positive sequence component as well as the magnitude and phase of negative sequence component, having a fine dynamic response property. Since the negative sequence of fundamental wave will not lead to two times harmonic component in the dual d-q frame and only have harmonic component, the low-pass filter design bandwidth is expanded and the filter delay is reduced. Consequently, without affecting the detecting precision, the dynamic response speed is improved.

II. D-Q TRANSFORMATION ANALYSIS IN HARMONIC AND THREE-PHASE UNBALANCE CONDITION

Let d-q transformation expression to be

$$\begin{bmatrix} u_d \\ u_q \end{bmatrix} = \sqrt{\frac{2}{3}} \begin{bmatrix} \cos\omega t & \cos(\omega t - 2\pi/3) & \cos(\omega t + 2\pi/3) \\ -\sin\omega t & -\sin(\omega t - 2\pi/3) & -\sin(\omega t + 2\pi/3) \end{bmatrix} \begin{bmatrix} u_a \\ u_b \\ u_c \end{bmatrix} \quad (1)$$

Suppose the 5th and the 7th harmonics are in grid, and total harmonic distortion (THD) rate is 18.03%, then voltage of phase A drops during 0.1s~0.6s, leading to three-phase unbalance. The remaining value of phase A is 156V. The d-q transformation result of three-phase voltages is shown in Fig.1.

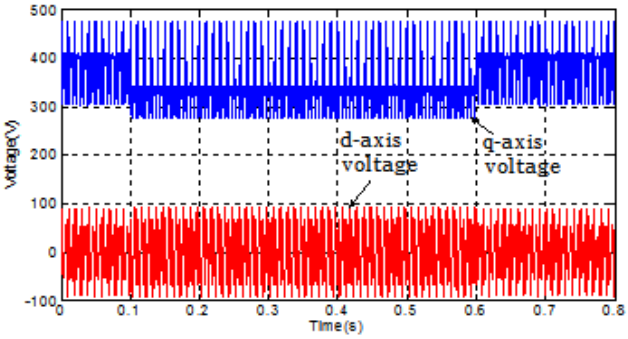

Figure 1. D-q transformation result of three-phase voltages under harmonic and unbalance condition

Table I is the spectrum analysis between 0.1s~0.6s from Fig.1. According to the spectrum analysis data, the second order harmonic caused by three-phase unbalance is one of the main harmonic components.

TABLE I
SPECTRUM ANALYSIS FOR D-Q TRANSFORMATION RESULTS OF THREE-PHASE VOLTAGES UNDER HARMONIC AND UNBALANCE CONDITION

harmonic order/k	2	3	4	5	6
d-axis voltage /V	26.9501	0.0191	40.4081	0.0006	26.9501
q-axis voltage /V	26.9233	0.0171	40.3986	0.0018	26.9421

In Fig.1, the d-q transformation results cannot be used directly in voltage sag characteristic analysis, because low-pass filtering is required. In this paper, the second order Butterworth filter [23] is used as low-pass filter (LPF). Being filtered by 40Hz low-pass filter, the d-q transformation result is shown in Fig.2.

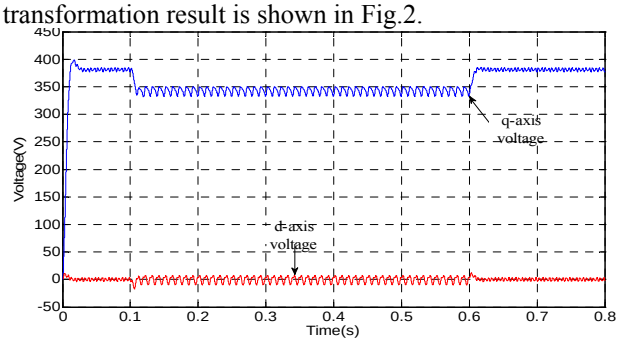

Figure 2. D-q transformation result by 40Hz low-pass filter

In the same way, suppose the harmonic condition is the same as above, but all the three-phase-balance voltages drop during 0.1s~0.6s, and the remaining value of each phase is 156V. Fig.3 is the d-q transformation result. Obviously, the harmonic spectrum analysis of Fig.3 does not include the second order harmonic component caused by three-phase unbalance, while the other harmonics analysis is similar to Table I. It is shown in Table II.

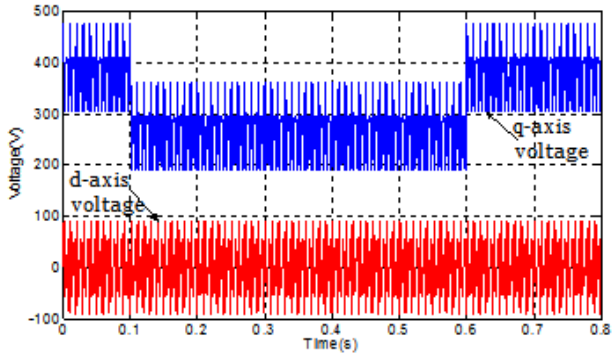

Figure 3. D-q transformation result of three-phase voltages under harmonic and balance condition

TABLE II
SPECTRUM ANALYSIS FOR D-Q TRANSFORMATION RESULT OF THREE-PHASE VOLTAGES UNDER HARMONIC AND BALANCE CONDITION

harmonic order/k	2	3	4	5	6
d-axis voltage /V	0.0059	0.0140	40.4091	0.0026	26.9505
q-axis voltage /V	0.0135	0.0206	40.4090	0.0027	26.9495

Similarly, the d-q transformation result cannot be used directly in voltage sag characteristic analysis and need low-pass filtering. Fig.4 is the d-q transformation result by 70Hz low-pass Butterworth filter.

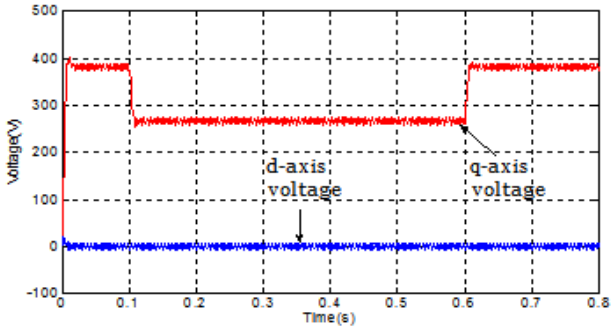

Figure 4. D-q transformation result by 70Hz low-pass filter

Comparing Fig.2 with Fig.4, their voltage-sag overshoots are ±13.26V and ±10.6V. The d-q transformation low-pass filtering results are similar, but the second one has a better step response and amplitude-frequency characteristic by using 70 Hz filter. Hence, without reducing detection precision, the three-phase unbalance elimination expands the design bandwidth of low-pass filter and reduces the low-pass filter delay.

III. DECOUPLING POSITIVE AND NEGATIVE SEQUENCES IN DOUBLE D-Q SYNCHRONOUS REFERENCE FRAME

Let the expression of three-phase system voltages (or currents) to be

$$\begin{cases} x_a = x_a^+ + x_a^- + x_0 + \sum_{k=2}^{n}\left(x_a^{k+} + x_a^{k-}\right) \\ x_b = x_b^+ + x_b^- + x_0 + \sum_{k=2}^{n}\left(x_b^{k+} + x_b^{k-}\right) \\ x_c = x_c^+ + x_c^- + x_0 + \sum_{k=2}^{n}\left(x_c^{k+} + x_c^{k-}\right) \end{cases} \tag{2}$$

In (2), x_a, x_b and x_c are three-phase voltages or currents; x_a^+, x_b^+ and x_c^+ are fundamental positive sequence components; x_a^-, x_b^- and x_c^- are fundamental negative sequence components; x_a^{k+}, x_b^{k+} and x_c^{k+} are positive sequence components of kth harmonic wave; x_a^{k-}, x_b^{k-} and x_c^{k-} are negative sequence components of kth harmonic wave; x_0 is zero sequence component.

Furthermore, let A expresses vector effective value, φ expresses phase angle, then can get:

$$\begin{cases} x_a^+ = \sqrt{2}A^+\sin(\omega t + \phi^+) \\ x_b^+ = \sqrt{2}A^+\sin(\omega t - 2\pi/3 + \phi^+) \\ x_c^+ = \sqrt{2}A^+\sin(\omega t + 2\pi/3 + \phi^+) \end{cases} \tag{3}$$

$$\begin{cases} x_a^- = \sqrt{2}A^-\sin(\omega t - \phi^-) \\ x_b^- = \sqrt{2}A^-\sin(\omega t + 2\pi/3 - \phi^-) \\ x_c^- = \sqrt{2}A^-\sin(\omega t - 2\pi/3 - \phi^-) \end{cases} \tag{4}$$

$$\begin{cases} x_a^{k+} = \sqrt{2}A^{k+}\sin(\omega_k t + \phi^{k+}) \\ x_b^{k+} = \sqrt{2}A^{k+}\sin(\omega_k t - 2\pi/3 + \phi^{k+}) \\ x_c^{k+} = \sqrt{2}A^{k+}\sin(\omega_k t + 2\pi/3 + \phi^{k+}) \end{cases} \tag{5}$$

$$\begin{cases} x_a^{k-} = \sqrt{2}A^{k-}\sin(\omega_k t - \phi^{k-}) \\ x_b^{k-} = \sqrt{2}A^{k-}\sin(\omega_k t + 2\pi/3 - \phi^{k-}) \\ x_c^{k-} = \sqrt{2}A^{k-}\sin(\omega_k t - 2\pi/3 - \phi^{k-}) \end{cases} \tag{6}$$

$$x_0 = \tfrac{1}{3}\left(x_a + x_b + x_c\right) \tag{7}$$

Convert (2) into α-β coordinate, so that:

$$\begin{bmatrix} x_\alpha \\ x_\beta \end{bmatrix} = \sqrt{\tfrac{2}{3}}\begin{bmatrix} 1 & -1/2 & -1/2 \\ 0 & \sqrt{3}/2 & -\sqrt{3}/2 \end{bmatrix}\begin{bmatrix} x_a \\ x_b \\ x_c \end{bmatrix} = C_{32}\begin{bmatrix} x_a \\ x_b \\ x_c \end{bmatrix} \tag{8}$$

Substitute (2) ~ (6) into (8), then get x_α, x_β:

$$\begin{cases} x_\alpha(t) = \sqrt{3}A^+\sin(\omega t + \phi^+) + \sqrt{3}A^-\sin(\omega t - \phi^+) \\ \qquad + \sum_{k=2}^{n}\left[\sqrt{3}A^{k+}\sin(\omega_k t + \phi^{k+}) + \sqrt{3}A^{k-}\sin(\omega_k t - \phi^{k-})\right] \\ x_\beta(t) = -\sqrt{3}A^+\cos(\omega t + \phi^+) + \sqrt{3}A^-\cos(\omega t - \phi^+) \\ \qquad + \sum_{k=2}^{n}\left[-\sqrt{3}A^{k+}\cos(\omega_k t + \phi^{k+}) + \sqrt{3}A^{k-}\cos(\omega_k t - \phi^{k-})\right] \end{cases} \tag{9}$$

Fig.5 gives the vector relationship between double d-q synchronous reference frame and *α-β* coordinate, Then we can transform x_α and x_β in *α-β* coordinate into x_{d+}, x_{q+} and x_{d-}, x_{q-} in double d-q synchronous reference frame.

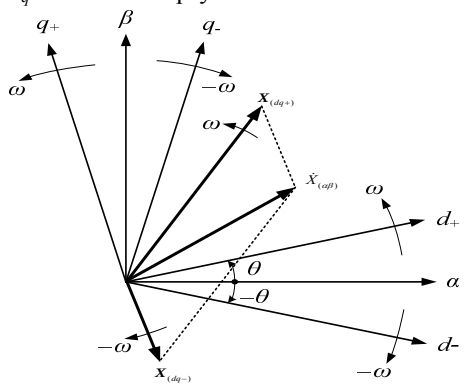

Figure 5. Vectors and axes of double synchronous reference frame

According to Fig. 5, the transformational matrix is:

$$\begin{bmatrix} x_{d+} \\ x_{q+} \end{bmatrix} = \begin{bmatrix} \cos\theta & \sin\theta \\ -\sin\theta & \cos\theta \end{bmatrix}\begin{bmatrix} x_\alpha \\ x_\beta \end{bmatrix} \tag{10}$$

$$\begin{bmatrix} x_{d-} \\ x_{q-} \end{bmatrix} = \begin{bmatrix} \cos(-\theta) & \sin(-\theta) \\ -\sin(-\theta) & \cos(-\theta) \end{bmatrix}\begin{bmatrix} x_\alpha \\ x_\beta \end{bmatrix} \tag{11}$$

According to (9)～(11), the mathematical description of three-phase system in double d-q synchronous reference frame is obtained.

Reference [2] adopts the transformational matrix shown in (10) and (11), and transforms x_α and x_β into double d-q synchronous reference frame. But fundamental components of $x_{d+}(x_{q+})$ and $x_{d-}(x_{q-})$ cannot be decoupled in this way, on the contrary, superposed frequency-doubled component of opposite phase sequence appears in the expressions. In fact, from (10) and (11), we can get:

$$\begin{bmatrix} x_{d+}^{+} \\ x_{q+}^{+} \end{bmatrix} = \begin{bmatrix} \cos\theta & \sin\theta \\ -\sin\theta & \cos\theta \end{bmatrix} \begin{bmatrix} x_{\alpha}^{+}(t) \\ x_{\beta}^{+}(t) \end{bmatrix} \tag{12}$$

$$\begin{bmatrix} x_{d-}^{-} \\ x_{q-}^{-} \end{bmatrix} = \begin{bmatrix} \cos\theta & -\sin\theta \\ \sin\theta & \cos\theta \end{bmatrix} \begin{bmatrix} x_{\alpha}^{-}(t) \\ x_{\beta}^{-}(t) \end{bmatrix} \tag{13}$$

In (12) and (13), x_{d+}^{+}, x_{q+}^{+}, x_{α}^{+} and x_{β}^{+} are fundamental positive sequence components; x_{d-}^{-}, x_{q-}^{-}, x_{α}^{-} and x_{β}^{-} are fundamental negative sequence components.

Apparently, x_{d+}^{+} (x_{q+}^{+}) and x_{d-}^{-} (x_{q-}^{-}) are decoupling. In order to get x_{α}^{+}, x_{β}^{+}, x_{α}^{-} and x_{β}^{-}, we can analyze x_{α} and x_{β} in fundamental positive and negative sequences. From (9), we find

$$\begin{aligned} \begin{bmatrix} x_{\alpha}(t) \\ x_{\beta}(t) \end{bmatrix} &= \begin{bmatrix} x_{\alpha}^{+}(t) \\ x_{\beta}^{+}(t) \end{bmatrix} + \begin{bmatrix} x_{\alpha}^{-}(t) \\ x_{\beta}^{-}(t) \end{bmatrix} + \begin{bmatrix} x_{\alpha}^{k+}(t) \\ x_{\beta}^{k+}(t) \end{bmatrix} + \begin{bmatrix} x_{\alpha}^{k-}(t) \\ x_{\beta}^{k-}(t) \end{bmatrix} \\ &= \sqrt{3}A^{+} \begin{bmatrix} \sin(\omega t+\phi^{+}) \\ -\cos(\omega t+\phi^{+}) \end{bmatrix} + \sqrt{3}A^{-} \begin{bmatrix} \sin(\omega t-\phi^{-}) \\ \cos(\omega t-\phi^{-}) \end{bmatrix} \\ &+ \sqrt{3} \begin{bmatrix} \sum_{k=2}^{n} A^{k+}\sin(\omega_k t+\phi^{k+}) \\ -\sum_{k=2}^{n} A^{k+}\cos(\omega_k t+\phi^{k+}) \end{bmatrix} + \sqrt{3} \begin{bmatrix} \sum_{k=2}^{n} A^{k-}\sin(\omega_k t-\phi^{k-}) \\ \sum_{k=2}^{n} A^{k-}\cos(\omega_k t-\phi^{k-}) \end{bmatrix} \end{aligned} \tag{14}$$

Let x_{α} and x_{β} from (14) delay for 0.005s (T/4), we can get:

$$\begin{aligned} \begin{bmatrix} x_{\alpha}(t-\frac{T}{4}) \\ x_{\beta}(t-\frac{T}{4}) \end{bmatrix} &= \begin{bmatrix} x_{\alpha}^{+}(t-\frac{T}{4}) \\ x_{\beta}^{+}(t-\frac{T}{4}) \end{bmatrix} + \begin{bmatrix} x_{\alpha}^{-}(t-\frac{T}{4}) \\ x_{\beta}^{-}(t-\frac{T}{4}) \end{bmatrix} + \begin{bmatrix} x_{\alpha}^{k+}(t-\frac{T}{4}) \\ x_{\beta}^{k+}(t-\frac{T}{4}) \end{bmatrix} + \begin{bmatrix} x_{\alpha}^{k-}(t-\frac{T}{4}) \\ x_{\beta}^{k-}(t-\frac{T}{4}) \end{bmatrix} \\ &= -\sqrt{3}A^{+} \begin{bmatrix} \cos(\omega t+\phi^{+}) \\ \sin(\omega t+\phi^{+}) \end{bmatrix} + \sqrt{3}A^{-} \begin{bmatrix} -\cos(\omega t-\phi^{-}) \\ \sin(\omega t-\phi^{-}) \end{bmatrix} \\ &+ \sqrt{3} \begin{bmatrix} \sum_{k=2}^{n} A^{k+}\sin(\omega_k t-\frac{k\pi}{2}+\phi^{k+}) \\ -\sum_{k=2}^{n} A^{k+}\cos(\omega_k t-\frac{k\pi}{2}+\phi^{k+}) \end{bmatrix} + \sqrt{3} \begin{bmatrix} \sum_{k=2}^{n} A^{k-}\sin(\omega_k t-\frac{k\pi}{2}-\phi^{k-}) \\ \sum_{k=2}^{n} A^{k-}\cos(\omega_k t-\frac{k\pi}{2}-\phi^{k-}) \end{bmatrix} \end{aligned} \tag{15}$$

From (14) and (15), we find:

$$\begin{aligned} \begin{bmatrix} x_{\alpha}^{+} \\ x_{\beta}^{+} \\ x_{\alpha}^{-} \\ x_{\beta}^{-} \end{bmatrix} &= \frac{1}{2} \begin{bmatrix} 1 & 0 & 0 & -1 \\ 0 & 1 & 1 & 0 \\ 1 & 0 & 0 & 1 \\ 0 & 1 & -1 & 0 \end{bmatrix} \begin{bmatrix} x_{\alpha}(t) \\ x_{\beta}(t) \\ x_{\alpha}(t-T/4) \\ x_{\beta}(t-T/4) \end{bmatrix} \\ &- \frac{1}{2}\sum_{k=2}^{n} \begin{bmatrix} x_{\alpha}^{k+}(t)+x_{\alpha}^{k-}(t)-x_{\beta}^{k+}(t-T/4)-x_{\beta}^{k-}(t-T/4) \\ x_{\beta}^{k+}(t)+x_{\beta}^{k-}(t)+x_{\alpha}^{k+}(t-T/4)+x_{\alpha}^{k-}(t-T/4) \\ x_{\alpha}^{k+}(t)+x_{\alpha}^{k-}(t)+x_{\beta}^{k+}(t-T/4)+x_{\beta}^{k-}(t-T/4) \\ x_{\beta}^{k+}(t)+x_{\beta}^{k-}(t)-x_{\alpha}^{k+}(t-T/4)-x_{\alpha}^{k-}(t-T/4) \end{bmatrix} \end{aligned} \tag{16}$$

After T/4 time-lapse elimination and low-pass filtering, from (16) we can get x_{α}^{+}, x_{β}^{+}, x_{α}^{-} and x_{β}^{-}, that are from fundamental positive and negative sequence components. Thus, we can get the decoupled x_{d+}^{+}, x_{q+}^{+}, x_{d-}^{-}, and x_{q-}^{-} in double d-q synchronous reference frame. That is why this paper calls the decoupling method "T/4 time-lapse elimination method".

IV. Structure Models of Three-Phase Magnitude-Phase Detection System

The decoupling progress of three-phase fundamental positive and negative sequence components in double d-q synchronous reference frame is shown in previous section. With (8), (12), (13), (15) and (16), block diagram of the three-phase magnitude-phase detection can be drawn as Fig.6.

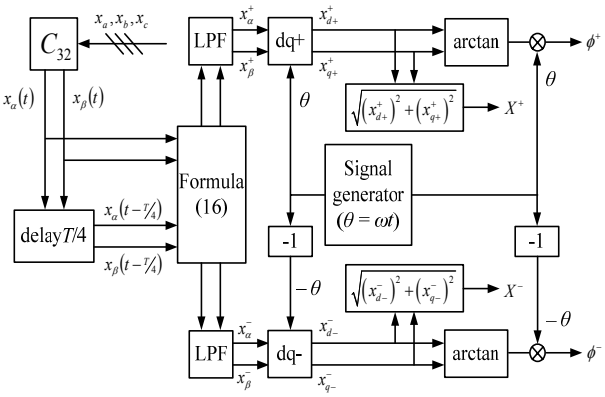

Figure 6. Block diagram of the three-phase magnitude-phase detection

In Fig.6, X^{+} is the fundamental positive sequence component magnitude, X^{-} is the fundamental negative sequence component magnitude; θ is offered by ramp signal generator, and LPF restrains harmonic disturbance in positive and negative sequence components. As a result of (16), we get

1) x_{α}^{+} (x_{β}^{+}) can restrain the negative sequence component of the kth harmonic wave;

2) x_{α}^{-} (x_{β}^{-}) can restrain the positive sequence component of the kth harmonic wave.

Unlike the principle in Fig. 6, reference [24] mentions T/16 time-lapse elimination detection method based on double synchronous reference frame, which also decouple the positive and negative sequences of fundamental component. But compared the two methods, T/4 time-lapse elimination method has superiority on harmonic suppression and phase detection. The details will be discussed in next section.

V. Simulation

To prove the feasibility of presented magnitude-phase detection method, simulation was finished. T/4 time-lapse elimination method compares with previous three-phase SPLL and T/16 time-lapse elimination method, transient response under normal grid condition, dynamic responses under three-phase unbalance with harmonic pollution condition and phase jump condition were obtained respectively.

A. Transient Response under Normal Grid Condition

Analyze the transient response of three methods under normal grid condition. Parameters: phase voltage effective value 220V, rated frequency 50Hz, with the 3rd and the 5th harmonic, THD rate 2.3%≤5.0%. After detecting the voltage magnitude and phase of three-phase fundamental wave, the simulation result as shown as the following Fig.7.

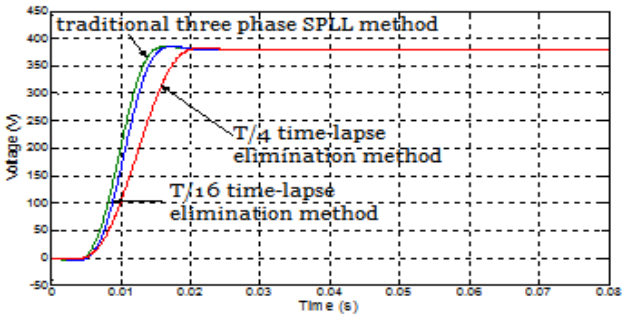

(a) Positive sequence voltage amplitude of three-phase fundamental wave

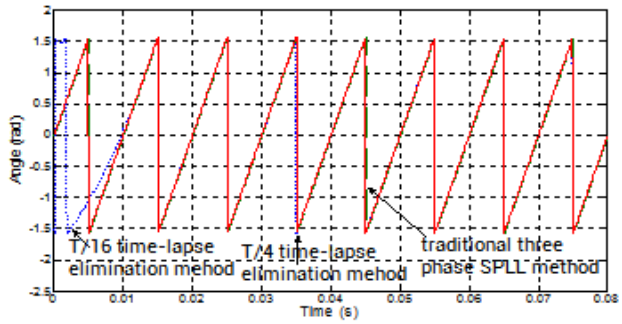

(b) Positive sequence phase position of three-phase fundamental wave

Figure 7. Response curves under normal grid condition

As shown in Fig.7(a), all the three transient overshoots under normal grid condition are approximate. But three-phase SPLL, which takes the least setting time, has the best transient response. The other two methods with time-lapse have more setting time, but the setting time don't exceed 5/4 frequency period. Fig.7(b) shows that in the first frequency period, T/16 time-lapse elimination method has an obvious wave distortion, while the wave shapes of the other two methods coincide mainly.

B. Dynamic Response under Harmonic and Unbalanced Condition

Fig.8 is the simulation result under three-phase unbalance with harmonic pollution condition. Parameters: phase voltage effective value 220V, rated frequency 50Hz, with the 3rd and the 5th harmonic, THD rate 25.01%, one phase voltage sag during 0.04s~0.1s and then three-phase unbalance.

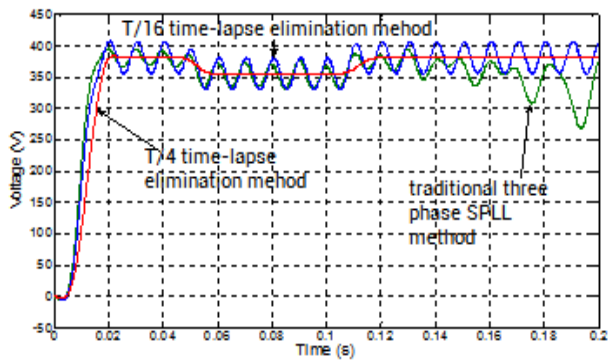

(a) Positive sequence voltage amplitude of three-phase fundamental wave

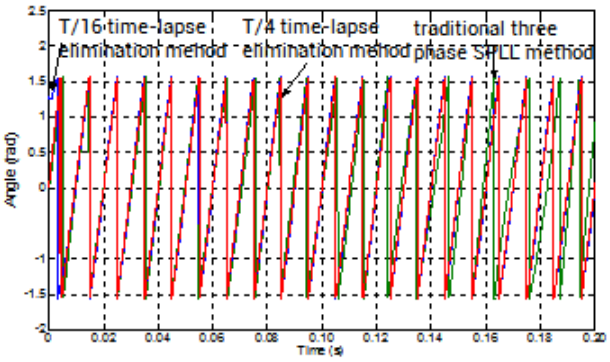

(b) Positive sequence phase position of three-phase fundamental wave

Figure 8. Dynamic response under harmonic and unbalanced condition

As shown in Fig.8, since voltage has unbalance disturbance with serious grid distortion, traditional three-phase SPLL cannot track the magnitude and phase of the fundamental positive sequence voltage; The T/16 time-lapse elimination method cannot suppress harmonic and its positive sequence voltage detection result has a bad steady state relative error is equal or greater than 5.0%; T/4 time-lapse elimination method, of which the relative steady state error of positive sequence voltage detection is equal or smaller than 0.5% and dynamic response time is 0.018s obtains a good dynamic response property. This simulation example verifies the analysis result of (16) in previous section, and explains that T/4 time-lapse elimination method can suppress odd harmonic and can track magnitude and phase of the fundamental positive sequence voltage under harmonic distortion condition.

C. Detection Result under Phase Jump of Three-phase Voltages

Parameters: phase voltage effective value 220V, rated frequency 50Hz, with the 3rd and the 5th harmonic, THD rate2.3%≤5.0%, three-phase voltage phase jumping at 0.045s, phase jump angle is -30°, system restoration at 0.16s. After detecting the fundamental positive sequence voltage magnitude and phase, the result is shown in Fig.9.

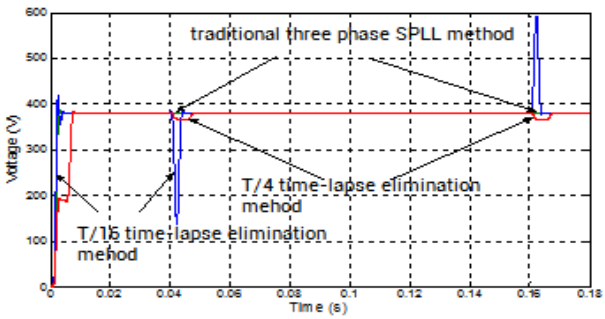

(a) Positive sequence voltage amplitude of three-phase fundamental wave

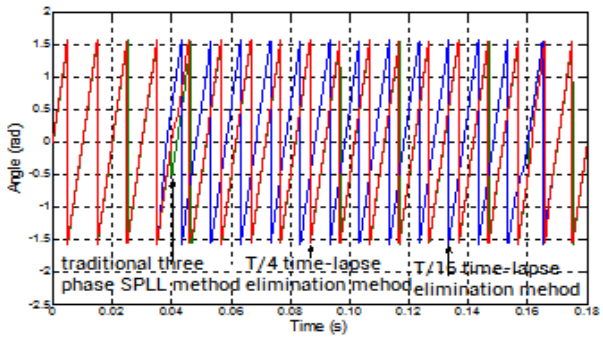

(b) Positive sequence phase position of three-phase fundamental wave

Figure 9. Dynamic response under phase jump of three-phase voltages

In Fig.9, the traditional three-phase SPLL method has the best real-time property on detecting three-phase voltage phase jump; T/4 time-lapse elimination detection method can detect phase jump although its real-time property is not 100% well; the T/16 time-lapse elimination detection method has obvious peak on the positive sequence voltage magnitude, and the phase position has obvious deviation.

VI. Conclusion

This paper introduces T/4 time-lapse elimination method, a novel magnitude-phase detection method based on double synchronous reference frame. This method achieves decoupling positive and negative sequences of fundamental wave with double d-q transformation and detects the magnitude and phase position of three-phase voltages (or currents) fundamental positive sequence component and negative sequence component respectively. Simulation results indicate that the novel method solves the problems in traditional three-phase SPLL circuits and even enjoys a high precision of measure. Compared with T/16 time-lapse elimination method, this method has superiority on harmonic suppression and phase tracking. Detecting system model based on this method is simple, and they can be used in occasion where harmonic distortion is heavy and three-phase unbalance, especially lots of application values exist in detecting voltage synchronous signal of wind energy generation system.

Acknowledgement

The authors also want to give their thanks to the Natural Science Foundation of China (No. 50967001) and Excellent Youth Teacher Foundation of Lanzhou University of Technology (No. Q200814).

References

[1] D. H. Huang, J. J. Chen and L. Zhang, "Impact of Large-scale Wind Power Integration on Power System," *Guangdong Electric Power*, Vol. 23, No. 7, pp. 27–30, July 2010.

[2] ZHOU Peng, HE Yikang, HU Jiabing, "Detection of voltage synchronization signals for a wind energy generation system unbalanced grid conditions," *Transactions of China Electro technical Society*, Vol. 23, No. 5, pp. 108-113, 2010.

[3] ZHU Xiaoguang, JIANG Xiaohua, "Weighted least square estimation algorithm with software phase-locked loop for voltage sag compensation by SMES," *Proceeding of 35th Annual IEEE Power Electronics Specialists Conference:* Vol. 3, pp. 2034-2038, 2004.

[4] L. H. Mou, J. Lv and W. Zhou, "Synchronous reference frame method for reactive and harmonics currents detection based on sequence components extraction," *Journal of Central South University (Science and Technology)*, Vol. 42, No. 2, pp. 419–426, 2011.

[5] Bin Liu, Shifei Yang, Lei Shi, et al, "Modeling of Failure Detector Based on Message Delay Prediction Mechanism," *Journal of Software,* Vol. 6, No. 9, pp. 1821–1828, 2011.

[6] WEN ZhiWei, HE ShiEn, "Analysis of Three-phase Magnitude-phase Detection Method Based on Double dq Transformation," *2012 IEEE 7th International Power Electronics and Motion Control Conference - ECCE Asia,* pp. 340–344, 2011.

[7] JOVCIC D, "Phase locked loop system for FACTS," *IEEE Transactions on Power Systems*, Vol. 18, No. 3, pp. 1116-1124, 2003.

[8] SHEN Baike, MWINYIWIWA B, ZHANG Yongzheng, et al, "Sensorless maximum power point tracking of wind by DFIG using rotor position phase lock loop (PLL)," *IEEE Transactions on Power Electronics*, Vol. 24, No. 4, pp. 942-951, 2009.

[9] Xiaoying Zhang, Zhizhuang Cheng, Xiaolan Wang and Zhiwei Wen, "A Magnitude-phase Detection Method for Grid-connected Voltage of Wind Power Generation System," *Proceedings of 2012 International Conference on Modeling, Identification and Control,* pp. 926–932, 2012.

[10] KARIMI-GHARTEMANI M, "A novel three-phase magnitude-phase-locked loop system," *IEEE Transactions on Circuits and Systems I: Regular Papers*, Vol. 53, No. 8, pp. 1792-1802, 2006.

[11] AIELLO M, CATALIOTTI A, COSENTINO V, et al, "Synchronization techniques for power quality instruments," *IEEE Transactions on Instrumentation and Measurement*, Vol. 56, No. 5, pp. 1511-1519, 2007.

[12] SALAMAH AM, FINNEY SJ, WILLIANS BW, "Three-phase phase-lock loop for distorted utilities," *IET Electric Power Applications*, Vol. 1, No. 5, pp. 937-945, 2007.

[13] SANTOS F R M, SEIXAS PF, CORTIZO P C, et al, "Comparison of three single-phase PLL algorithms for UPS applications," *IEEE Transactions on Industrial Electronics*, Vol. 55, No. 8, pp. 2923-2932, 2008.

[14] SHINJI S, "A robust single-phase PLL system with stable and fast Tracking," *IEEE Transactions on Industry Applications*, Vol. 44, No. 2, pp. 624-633, 2008.

[15] AWAD H, SVENSSON J, BOLLEN M J, "Tuning software phase-locked loop for series-connected converters," *IEEE Transactions on Power Delivery*, Vol. 20, No. 1, pp. 300-308, 2005.

[16] ROLIM LGB, DA COSTA DR, AREDES M, "Analysis and software implementation of a robust synchronizing PLL circuit based on the pq theory," *IEEE Transactions on Industrial Electronics*, Vol. 53, No. 6, pp. 1919-1926, 2006.

[17] ZANUSO M, TASCA D, LEVANTINO S, et al, "Noise analysis and minimization in bang-bang digital PLLS," *IEEE Transactions on Circuits and Systems II: Express Briefs*, Vol. 56, No. 11, pp. 835-839, 2009.

[18] FREIJEDO F D, DOVAL-GANDOY J, LOPEZ O, et al, "Tuning of phase-locked loops for power converters under distorted utility conditions," *IEEE Transactions on Industry Applications*, Vol. 45, No. 6, pp. 2039-2047, 2009.

[19] LEE Jaewook, MOON Jaekyun, ZHANG Tong, et al. "New phase-locked loop design understanding the impact of a phase-tracking channel detector," *IEEE Transactions*

on Magnetics, Vol. 46, No. 3, pp. 830-836, 2010.
[20] S.J. Lee, M. Kim and S. K. Sul, "A novel control algorithm for static series compensators by use of PQR instantaneous power theory," *EEE Transactions on Power Electronics*, Vol. 19, No. 3, pp. 814–827, 2010.
[21] AIELLO M, CATALIOTTI A, NUCCIO S, "A chirp-z transform-based synchronizer for power system measurements," *IEEE Transactions on Instrumentation and Measurement*, Vol. 54, No. 3, pp. 1025-1032, 2005.
[22] GUO Wenyong, ZHAO Caihong, ZHANG Zhifeng, et al, "A novel three-phase magnitude-phase-lock loop system based on extended variable step size least mean square algorithm," *Automation of Electric Power Systems*, Vol. 32, No. 11, pp. 77-81, 2008.
[23] W. Wu, J. Y. Liu and Y. B. Liu, "Research summary of intelligent sales and marketing of smart grid," *Electric Power Automation Equipment*, Vol. 30, No. 5, pp. 131–135, May 2010.
[24] ZHOU Peng, HE Yikang, SUN Dan, et al, "Control and protection of a DFIG-based wind turbine under unbalanced grid voltage dips," *Proceeding of IEEE Industry Applications Society Annual Meeting*, pp. 1-8, 2008.

Xiaoying Zhang was born in Sichuan Province, China, in 1973. She is currently an associate professor at Lanzhou University of Technology, Gansu, China. She obtained a first class BEng degree in 1998 and a Master's degree in 2001 from Xi'an University of Technology, P R China. Her research interests include the stability of power system, wind power generation control.

Zheng Jiang was born in Anhui Province, China, in1987. He is currently a graduate student at Lanzhou University of Technology, Gansu, China. He received his BEng degree in electrical engineering and automation from Wuhan University in 2008. His research interests include the voltage stability of power system, sensitivity analysis in power system.

Ning Ding was born in Shandong Province, China, in1988. He is currently a graduate student at Lanzhou University of Technology, Gansu, China. He received his BEng degree in electrical engineering and automation from Wuhan Polytechnic University in 2010. His research interests include the stability of power system, flow calculation of power system.